1460 *Biochemistry* **2010,** *49,* 1460–1468
DOI: 10.1021/bi901896b

BIOCHEMISTRY
including biophysical chemistry & molecular biology
Article

The Noncanonical Disulfide Bond as the Important Stabilizing Element of the Immunoglobulin Fold of the Dr Fimbrial DraE Subunit†

Rafał Piątek,*,‡ Piotr Bruździak,§ Marek Wojciechowski,∥ Beata Zalewska-Piątek,‡ and Józef Kur‡

‡*Department of Microbiology, Gdańsk University of Technology, ul. Narutowicza 11/12, 80-233 Gdańsk, Poland,*
§*Department of Physical Chemistry, Gdańsk University of Technology, ul. Narutowicza 11/12, 80-233 Gdańsk, Poland, and*
∥*Department of Pharmaceutical Technology and Biochemistry, Gdańsk University of Technology, ul. Narutowicza 11/12, 80-233 Gdańsk, Poland*

Received November 5, 2009; Revised Manuscript Received December 20, 2009

ABSTRACT: Fimbrial adhesins of pathogenic bacteria are linear protein associates responsible for binding to the specific host cell receptors. They are assembled via the chaperone/usher pathway conserved in Gram-negative bacteria. These adhesive organelles are characterized by the high resistance to dissociation and unfolding caused by temperature or chemical denaturants. The self-complemented (SC) recombinant subunits of adhesive structures make up the minimal model used to analyze stability phenomena of these organelles. The SC subunits are both highly stabilized thermodynamically and kinetically. They are characterized by a standard free energy of unfolding of 70−80 kJ/mol and a rate constant of unfolding of 10^{-17} s^{-1} (half-life of unfolding of 10^8 years at 25 °C). The DraE subunit of Dr fimbriae is characterized by a disulfide bond that joins the beginning of the A1 strand with the end of the B strand. Such localization is unique and differentiates this protein from other proteins of the Ig-like family. Sequence analysis shows that many protein subunits of adhesive structures possess cysteines that may form a potential disulfide bond homologous to that of DraE. In this paper, we investigate the influence of this noncanonical disulfide bond on the stability of DraE-sc by constructing a DraE-sc-ΔSS mutant protein (Cys/Ala mutant). This construct unfolds thermally at a T_m of 65.4 °C, more than 20 °C lower than that of the native DraE-sc protein, and possesses a different unfolding mechanism. The calculated standard free energy of unfolding of DraE-sc-ΔSS is equal to 30 ± 5 kJ/mol. This allows us to suggest that the disulfide bond is an important stabilizing feature of many fimbrial subunits.

The pili and fimbriae are surface-located adhesive structures expressed by most Gram-negative pathogens. They are crucial in recognition of the host tissue specific receptor particles. Initial binding to the receptor results in promotion of pathogenesis that besides tight attachment often involves bacterial invasion of the host cells and biofilm formation. Among them, the best characterized are the adhesive organelles expressed by the chaperone/usher machinery (*1*, *2*). Type P and 1 pili encoded by uropathogenic *Escherichia coli* strains are heteropolymeric protein complexes with a rodlike morphology. In these structures, the single adhesive subunit is located on the flexible fibrillum tip that protrudes from the long rigid helical rod (*3*). Caf1 is the protein subunit of the F1 surface antigen of *Yersinia pestis*, the causative agent of the plague. This homopolymeric adhesin morphologically forms an amorphous capsule (*4*, *5*). The Dr fimbriae are thin hairlike homopolymeric structures 2 nm in diameter composed of the DraE[1] protein (*6*−*10*). DraE is a building block of the Dr adhesin and promotes adhesion by interaction with host cell receptors: DAF glycoprotein and collagen type IV (*6*, *11*−*15*). At the tip of the Dr fimbriae, the DraD protein is localized, and it loosely interacts with the top DraE protein and may easily dissociate. Thus, DraD may exist in a form that is not attached to the fimbriae and persist in the bacterial capsule (*16*−*18*). The DraD protein is an important factor in the promotion of bacterial invasion of the host cell.

Although the adhesive structures mentioned above differ morphologically, they are all assembled via the highly conserved chaperone/usher pathway. All adhesive organelles are encoded by operons characterized by a similar organization. Each one is composed of four classes of genes encoding proteins engaged in operon expression regulation, the specific chaperone, the outer membrane usher, and the subunits of adhesive structure (*1*, *2*, *19*−*21*). There are many structural data that explain the mechanism of adhesive organelle formation by the chaperone/usher pathway (*19*, *22*−*27*). All subunits possess an Ig-like structure composed of six β-strands forming a β-sandwich. The fold is defective because it lacks a seventh C-terminal strand that occurs in classical stable Ig structures. Consequently, protein subunits cannot fold spontaneously and are prone to degradation after translocation to the periplasm. However, this structural defect is crucial for the mechanism of adhesin biogenesis. The chaperone in the periplasm forms with the subunit a specific soluble complex with a 1:1 stoichiometry. In this complex, the functionally conserved donor strand from the chaperone completes the

†This work was supported by the Polish Ministry of Science and Higher Education (Grant 2218/B/PO1/2008/34).

*To whom correspondence should be addressed: Department of Microbiology, Gdańsk University of Technology, ul. Narutowicza 11/12, 80-233 Gdańsk, Poland. Telephone: +48 58 347 24 17. Fax: +48 58 347 24 17. E-mail: wejraf@o2.pl.

[1]Abbreviations: C_p^{ex}, excess heat capacity; COG, Clusters of Orthologous Groups database; DraE, adhesive subunit of Dr fimbriae; DraE-sc, self-complemented DraE subunit; DraE-sc-ΔSS, DraE-sc mutant lacking a disulfide bond; DSC, differential scanning calorimetry; ΔC_p, heat capacity change of protein unfolding; ΔG, free energy change of protein unfolding; FT-IR, Fourier transform infrared spectroscopy; PDB, Protein Data Bank; PFAM, Protein Family database; rmsd, root-mean-square deviation; T_m, protein melting temperature.

 Published on Web 01/18/2010

Ig-like structure of the subunit by closing its acceptor cleft, the donor strand complementation (DSC) reaction (*5*, *19*, *28*, *29*). Formation of a functional adhesive structure proceeds through the usher protein located in the outer membrane via the donor strand exchange mechanism (DSE). At this step, the N-terminally located donor strand of one subunit completes the Ig fold of the subunit that proceeds it in formation of the protein associate (*5*, *19*, *22*, *24*). Therefore, at each step of this pathway, the incomplete structure of the subunit is stabilized by the donor strand introduced in trans from the chaperone or from the neighboring subunit. The paradox connected with energy sources needed for fiber formation was solved by Sauer et al. (*23*) and Zavialov et al. (*24*, *30*).

Although the structural background and energetic background of the fiber formation are very well recognized, the mechanism of the enormously high kinetic stability of fimbrial structures is under debate (*30*−*34*). In this paper, we indicate that the presence of a disulfide bond in the noncanonical position is a structural feature determining the enormously high observed stability of the DraE protein. Finally, we speculate that this bond may be also important in the stabilization of other subunits of adhesive structures containing a disulfide bond homologous to the one in the DraE protein.

EXPERIMENTAL PROCEDURES

Sequence Analysis. The prediction of the distribution of a disulfide bond, homologous to that of DraE in the whole family of fimbrial proteins (FP), was generated using PFAM (*35*) and Clusters of Orthologous Groups (COG) (*36*). To clarify and organize the analysis, we used phylogenetic division of gene clusters encoding adhesive structures of chaperone/usher systems proposed by Nuccio and Bäumler (*37*). This classification consists of six clades: α, β, γ (including $\gamma1-\gamma4$), κ, π, and σ. The α clade includes adhesive structures of the alternate chaperone/usher family. The σ clade includes structures of the archaic chaperone/usher family. The γ, κ, and β clades include well-characterized functionally and structurally adhesive structures of the classical chaperone/usher family. The β clade is a small clade of putative fimbrial operons belonging to classical chaperone/usher family. The protein subunits of adhesive structures comprising clades are characterized by specific conserved domain entries in PFAM or COG (*37*): α, PFAM04449; β, PFAM06551; γ($\gamma1$, $\gamma2$ $\gamma4$); π, PFAM00419 and COG3539; $\gamma3$, PFAM04619, PFAM06443, and PFAM05775; κ, PFAM00419, PFAM02432, and COG3539; σ, COG5430. Protein sequences comprising each PFAM or COG family were aligned independently to determine the occurrence of cysteine residues that may form a potential disulfide bond, homologous to that in DraE. In the case of PFAM00419 and COG3539, the reduced nonredundant subset of sequences was analyzed. Only sequences with more than 90 residues and not more than 90% identical to each other were included in the subset. The sequence analyses were prepared using Internet web scripts working in PFAM and COG. The $\gamma3$ clade is complex and mainly contains adhesive structures composed of protein subunits without a conserved domain signature. Gene clusters encoding such proteins were analyzed manually to determine the frequency of a potential disulfide bond. Prepared analysis is general and permits description of the propagation of protein subunits with potential disulfide bonds (with homologous localization to the DraE) in the context of the whole family of FPs divided into phylogeneticaly related clades.

Protein Expression, Purification, and Sample Preparation. DraE-sc-ΔSS (self-complemented) is a recombinant fusion protein derivative of DraE-sc in which two cysteine residues forming a native protein disulfide bond are replaced with alanine. Expression plasmid pET30-DraE-sc-ΔSS encoding DraE-sc, the mutant lacking a disulfide bond, was created on the basis of the pET30-DraE-sc plasmid described previously (*34*). The PCR-borne site-directed mutagenesis kit (Stratagene) was used to change codons encoding Cys to those encoding Ala. The DraE-sc-ΔSS protein was produced in the *E. coli* BL21(DE3)/pET30-DraE-sc-ΔSS strain and subsequently purified using procedures identical to those in the case of the DraE-sc protein (*34*). Finally, the purified protein was extensively dialyzed against 20 mM phosphate buffer (pH 7.5) and 100 mM NaCl. After dialysis, the buffer was stored as the reference buffer for microcalorimetry. In microcalorimetry experiments, the DraE-sc-ΔSS protein was concentrated using an Amicon Ultra concentrator (Millipore, Bedford, MA) to a final concentration of ca. 1 mg/mL. For FT-IR analysis, DraE-sc-ΔSS was further dialyzed against 10 mM phosphate buffer (pH 7.5), and then 10 mL of the protein sample, at a concentration of 1 mg/mL, was lyophilized.

SDS−*Polyacrylamide Gel Electrophoresis Assay*. Samples prepared for electrophoresis contained approximately 5−10 μg of the DraE-sc or DraE-sc-ΔSS protein in 1× Laemmli buffer (containing 1% SDS). Before electrophoresis, samples were unheated or heated for 10 min at 30, 40, 50, 60, 70, 80, 90, and 100 °C. Electrophoresis was performed in 15% polyacrylamide gels in running buffer [0.1% SDS and Tris-glycine (pH 8.3)]. After electrophoresis, gels were stained using Coomassie blue.

Microcalorimetry. DSC experiments were performed on the CSC 6300 Nano-DSC III differential scanning microcalorimeter (Calorimetry Sciences Corp., Lindon, UT) with a capillary cell volume of 0.299 mL in the temperature range from 10 to 90 °C. The experimental data were recorded using DSCRun (Calorimetry Sciences Corp.). The concentration of DraE-sc-ΔSS (molecular mass of 16.3 kDa) was ca. 1 mg/mL in each experiment. The analysis was performed with a scanning rate of 1 °C/min. Samples preparation, measurements, and data analysis were performed as described previously for the DraE-sc protein (*34*).

FT-IR Spectroscopy. All spectra were recorded with a Nicolet 8700 spectrometer (Thermo Electron Scientific Inc., Waltham, MA) using an electrically heated transmission cell (Harrick Scientific Products Inc., Pleasantville, NY) with CaF_2 windows and 56 μm Teflon spacers. Approximately 3 mg of lyophilized DraE-sc- ΔSS protein was dissolved in D_2O (final concentration of ca. 20 mg/mL) 1 h before the experiment to allow all accessible hydrogen atoms to exchange with deuterium. Sample manipulation, measurements, and data analysis were performed according to the protocol described previously for the DraE-sc protein (*34*).

Molecular Dynamics Simulations. The starting coordinates of both molecules were based on the Protein Data Bank NMR structure 1rxl. The version without a disulfide bond was modeled via replacement of both cysteines with alanines. GROMACS version 4.05 and its utilities were used for the system preparation and analysis (*38*). The following protocol was used for calculations concerning DraE-sc as well as the DraE-sc-ΔSS structure. The protein molecule was immersed in a cubic box of pre-equilibrated water. The size of the box was made sufficiently large to keep the distance between the solute and the box at 15 Å. The resulting number of water molecules in the system was 18870

with simulation box dimensions of 94, 70, and 89 Å for *x*, *y*, and *z*, respectively. The simulations were performed in NPT ensemble with the GROMOS43a2 force field, SPC water model, and periodic boundary conditions. Before the actual simulation, the entire system was first energy-minimized and then relaxed with a molecular dynamics run for 50 ps, with position restraints set to all protein heavy atoms while water molecules were allowed to move. The following production simulation was run for 80 ns, with a time step of 2 fs that was possible due to all bonds being fixed with the LINCS algorithm. Neighbor list and long-range forces were updated every five steps. Long-range interactions were calculated with PME (particle mesh Ewald).

The rate of hydrogen to deuterium exchange was estimated via examination of the hydrogen bond creation of particular protein backbone amide groups with the solvent during the simulation. As long as the group was shielded from solvent and there was no hydrogen bond to any of the water molecules, we assumed it was unexchanged. At the moment the first hydrogen bond appeared, this group was marked as exchanged and excluded from further analysis.

Since it is not possible to run the molecular dynamics for a sufficiently long time to see the actual protein denaturation, the calculations were repeated over the whole range of temperatures: 300, 310, 340, 370, 410, and 473 K.

RESULTS

Distribution of a DraE-like Disulfide Bond in the Family of Fimbrial Subunits of Chaperone/Usher Systems. The topology of the subunits of adhesive structures of the chaperone/usher type belonging to the fimbrial protein family resembles the incomplete Ig-like fold. Generally, it is composed of six β-strands forming a β-sandwich of two sheets with Greek-key topology and missing the seventh G strand donated by another subunit, thus completing the canonical seven-stranded Ig fold (*10*). Like in most members of the Ig superfamily, many of the fimbrial proteins possess a disulfide bond joining two β-strands, though the position of this bond is quite unusual and differs from that of the classical Ig family structures. In the canonical Ig fold, the disulfide bond binds β-strands B and F of opposite β-sheets and is located near the core of the protein, between the B3 and F3 positions (*39*). In the DraE subunit, the bond joins two adjacent β-strands, the beginning of strand A1 with the end of the strand B, and is placed at the top of the protein (Figure 1). An identically positioned disulfide bond exists in other determined structures of fimbrial subunits, including major [PapA (*26*) and FimA], minor [PapE (*23*), PapH (*40*), PapK (*19*), FimF (*27*), and FimG (*33*)], and FimH (*22*) pilin domains of tip adhesive subunits of heteropolimeric P and type 1 pili, AfaE-III (*9*), and DaaE (*15*) subunits of the Dr family of adhesins (Figure 1B). To estimate conservation of the DraE-like disulfide bond in the whole family of fimbrial subunits, we performed protein sequence analysis. On the basis of the similarities of usher protein sequences, the operons encoding adhesive structures are clustered in six main phylogenetic clades: α, β, γ (including $\gamma1-\gamma4$), κ, π, and σ (*37*). The α clade includes fimbrial structures of the alternate chaperone/usher system. Subunits building α-fimbriae are characterized by protein-conserved domain PFAM04449 and do not possess in their sequence cysteine residues that may form a potential disulfide bond. In the phylognetic analysis performed by Nuccio and Bäumler (*37*), the α clade is represented by 16 operons from a total of 189 investigated. The σ-fimbriae belong to archaic chaperone/usher systems [39 operons in the analysis of Nuccio and Bäumler (*37*)] and are composed by subunits with homology to the COG5430 conserved protein domain. Examples of this are adhesive structures encoded by the *csu*(*A*/*B*)*ABCDE* gen cluster of *Acinetobacter baumannii* (*41*). Protein subunits CsuA/B, CsuA, and CsuB possess in sequence two cysteine residues that may form a potential disulfide bond homologous to that of the DraE protein. These cysteine residues are well conserved in all σ-fimbriae subunits of the COG5430 family. The remaining clades (β, π, γ, and κ) are comprised of adhesive structures belonging to classical chaperone/usher systems. The β clade is represented in the publication of Nuccio and Bäumler by only five operons. The β-fimbriae are composed of subunits characterized by the PFAM06551 protein domain. Almost all β-subunits possess two conserved cysteine residues that may form a potential disulfide bond homologous to that of DraE. Most subunits of adhesive structures belonging to the $\gamma1$ (including type 1 pili of *E. coli*), $\gamma2$ (including 987P fimbriae of *E. coli*), $\gamma4$ (including Hif pili of *Haemophilus influenzae*), and π (including P pili of *E. coli*) clades are characterized by the PFAM00419 (Fimbrial family) conserved protein domain. In the PFAM, this family comprises 296 nonredundant sequences; 90% of them possess two conserved cysteines that may form a potential disulfide bond homologous to that in DraE. In the publication of Nuccio and Bäumler (*37*), these four clades comprise 105 operons. The κ clade [seven operons in the analysis of Nuccio and Bäumler (*37*)] is represented by *E. coli fae* gene clusters encoding F4 fimbriae composed of the main protein FaeG that possesses the PFAM02432 conserved domain (*42*). In the structure of FaeG and sequences of other proteins that comprise the PFAM02432 family, there are no cysteine residues forming disulfide bonds. The $\gamma3$ clade [15 operons in the analysis of Nuccio and Bäumler (*37*)] is the most divergent group, in the context of disulfide bond occurrence in protein subunits of adhesive structures. To this clade belong adhesive structures mentioned below assembled with the assistance of FGL chaperones (ref *10* and

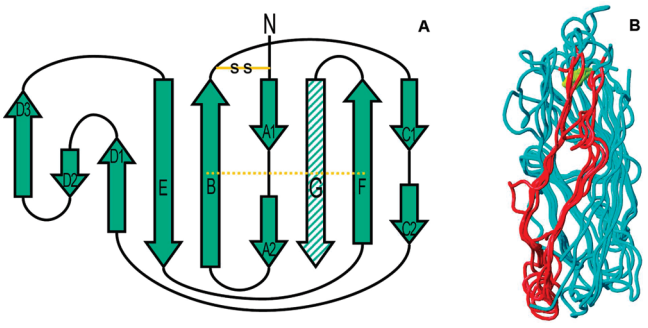

FIGURE 1: Unique position of the disulfide bridge in the DraE fimbrial protein. (A) Simplified topological diagram of the DraE-sc protein: S−S, noncanonical disulfide bond connecting ends of adjacent β-strands A and B in the structure of DraE and other fimbrial proteins; dashed line, canonical disulfide bond connecting β-strands B and F, characteristic of most proteins of the Ig superfamily; striped strand, N-terminal donor strand of DraE introduced as a C-terminal fusion peptide. (B) Superimposed structures of five selected proteins of the fimbrial family: PapA (PDB entry 2uy6), FimA (PDB entry 2jby), PapK (PDB entry 1pdk), FimG (PDB entry 3bfq), and DraE (PDB entry 1rxl). PapA and FimA are major and PapK and FimG minor subunits of P and type 1 pili belonging to clades π and $\gamma1$, respectively. The DraE adhesin subunit of Dr fimbriae represents the $\gamma4$ clade. Disulfide bonds are drawn as sticks. The first two adjacent β-strands, A and B, joined by the disulfide bridge are colored red. Superposition of the structures was calculated with MultiProt (*52*) and visualized with Rasmol.

references cited therein). The protein subunits encoded by *E. coli* gene clusters *dra* (adhesive structure, Dr fimbriae; fimbrial subunit, DraE), *daa* (F1845 fimbriae, DaaE), *agg* (AAF/I fimbriae, AggA), *aaf* (AAF/II fimbriae, AafA), *agg-3* (AAF/III fimbriae, Aag3A), *dafa* (diffuse adherence fibrillar adhesion, DafaE), *afa-3* (afimbrial adhesin Afa-III, AfaE-III), and *afa-8* (afimbrial adhesin Afa-VIII, AfaE-VIII) possess two conserved cysteine residues forming a disulfide bond. These operons also encode invasin subunits that in the case of AfaE-III and Dr adhesins are located at the tip of the fiber (*8*, *43*). Invasin proteins possess two cysteine residues that form a disulfide bond that is not homologous to that of DraE. In DraD and AfaD structures, this bond connects strands B and F. The *Y. pestis* and *Yersinia enterocolitica* contain similarly organized gene clusters *psa* and *myf*, respectively, which encode fimbrial antigen pH6 and Myf fimbriae, respectively. Fimbrial subunits of these structures do not possess cysteine residues. The *caf* gene cluster of *Y. pestis* encodes the F1 capsular antigen composed of Caf1 subunits that do not possess a disulfide bond (*24*). The subunits encoded by gene clusters *cs6-1* (adhesive structure, colonization factor CS6-1; protein subunits, CS6-1A and CS6-1B), *cs6-2* (colonization factor CS6-2; CS6-2A and CS6-2B), *saf* (atypical fimbriae Saf; SafA and SafD), *sef* (SEF14 fimbriae; SefA and SefD), and *css* (CS6 fibrillae; CssA and CssB) do not possess potential disulfide bonds (*44*, *45*). The SafD and SefD proteins belong to the PFAM05775 conserved domain to which also belong invasins of Dr family, mentioned above.

The analysis presented here shows that many protein subunits of adhesive structures of the chaperone/usher system possess cysteine residues that may potentially form such a typical localized disulfide bond homologous to that of DraE. Further, this bond is strictly conserved within the family of Dr adhesins (PFAM04619). We conclude that data presented in this paper, considering the influence of this disulfide bond on the stability of the DraE, permit us to speculate about its importance for the stability of other subunits of adhesive structures.

Disulfide Bond Lacking Mutant of DraE-sc Lost SDS Resistance. The physical basis of protein kinetic stability is poorly understood, and no general mechanisms have been implicated in this phenomena. Kinetically stable proteins under native conditions are characterized by very poor participation of partially unfolded structures (*46*). This leads to high resistance of such proteins to proteolytic degradation (*46*, *47*). Kinetically stable proteins are also often resistant to chemical denaturation, for example, by sodium dodecyl sulfate (SDS). One of the simplest methods for determining protein kinetic stability is to measure the resistance of the native protein structure to denaturation by SDS under the conditions used for SDS−polyacrylamide gel electrophoresis (SDS−PAGE) (*48*). The assay is based on the comparison of gel migration of boiled and unboiled protein samples prepared in the Laemmli buffer (containing SDS). Proteins that migrate in gel at the same level in boiled and unheated samples are depicted as SDS nonresistant and exhibit rather low kinetic stability. In contrast, kinetically stable proteins in samples incubated at room temperature migrate slower on the gel than the same protein boiled before electrophoresis. The observed retardation is connected with a decrease in the level of SDS binding to the nativelike globular form of the protein. The native protein−SDS complex possesses a lower negative charge in contrast to the totally thermally denatured protein saturated with SDS particles.

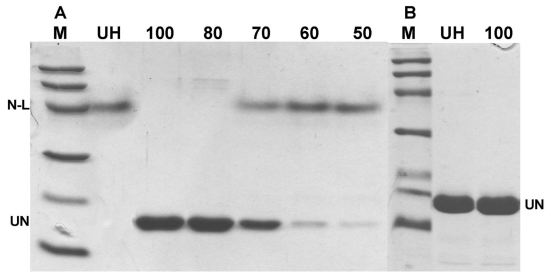

FIGURE 2: SDS resistance assay of the DraE-sc and the DraE-sc-ΔSS proteins. SDS−PAGE assay of SDS resistance of (A) the DraE-sc and (B) DraE-sc-ΔSS fimbrial proteins. Protein samples were either unheated (UH) or heated at 50, 60, 70, 80, and 100 °C for 10 min immediately prior to being loaded onto the gel: UN, unfolded form of the protein, with a band at ca. 16 kDa; N-L, nativelike form of the protein, with a band at ca. 45 kDa; M, low-molecular mass calibration kit for SDS electrophoresis [97, 66, 45, 30, 20.1, and 14.4 kDa (GE Healthcare)].

The chaperone/usher type adhesive structures are known from their resistance to SDS. Type 1 and P pili need to be boiled under acidic conditions for complete dissociation (*49*, *50*). The Dr fimbriae boiled in a Laemmli buffer show on gels many high-molecular mass bands that correspond to the incompletely dissociated adhesion structures (*7*). Also, the minimal form of Dr fimbriae, the self-complemented DraE subunit (DraE-sc), is highly resistant to SDS unfolding. The DraE-sc protein incubated in Laemmli buffer at room temperature is almost quantitatively retarded in gel electrophoresis (band on the level of 45 kDa) (Figure 2A). The retardation effect is observed even in samples incubated for 10 min in Laemmli buffer at 70 °C. This simple experiment correlates quite well with the results of the DraE-sc denaturation experiments using DSC microcalorimetry and FT-IR spectroscopy (*34*). The disulfide bond lacking mutant of DraE-sc characterized in this work totally lost SDS resistance. DraE-sc-ΔSS incubated in Laemmli buffer at room temperature migrates in a manner on the gel identical to that of the protein sample that was boiled for 10 min (Figure 2B). The presented SDS resistance assay clearly shows that deletion of a disulfide bond from DraE-sc results in a loss of kinetic and thermal stability.

Changes in the Mechanism of DraE-sc-ΔSS Denaturation Caused by Mutation. A series of differential scanning microcalorimetry (DSC) experiments with the DraE-sc-ΔSS protein has been performed at a scan rate of 1 °C/min, under buffer condition identical to those for the case of DraE-sc (*34*). These experiments allowed us to indicate differences between denaturation of previously described DraE-sc and its mutant lacking a disulfide bond, DraE-sc-ΔSS. First, the denaturation process of DraE-sc-ΔSS is reversible, in contrast to that of DraE-sc whose transition is almost completely irreversible (*34*). To estimate the level of reversibility, we performed the DSC experiment by interrupting the heating of the sample in following regions of the transition peak and subsequently cooled the sample to the initial temperature of the scan (Figure 3). The obtained endothermic reheating peaks correspond to ∼95% of the initial peak areas, if heating is stopped directly after the transition. Even if the samples were overheated outside the transition peak, up to 85 °C, the observed reversibility in reheating scan was ca. 75% (Figure 3). We concluded that the direct use of a simple two-state equilibrium model in the case of DraE-sc-ΔSS is acceptable. This statement is supported by the additional characteristics of heat capacity transition curves that clearly show that the observed insignificant irreversibility is connected with the kinetic process,

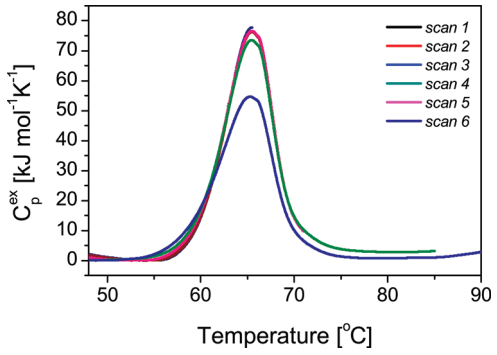

FIGURE 3: Reversibility of the DraE-sc-ΔSS denaturation. First DSC scan (black line) and the next reheating scans (other colors) of the DraE-sc-ΔSS protein interrupted at different temperatures in the region of the transition. The last scan (dark blue), after reheating to 85 °C, exhibits a lower enthalpy of transition that is connected with irreversible processes occurring at higher temperatures.

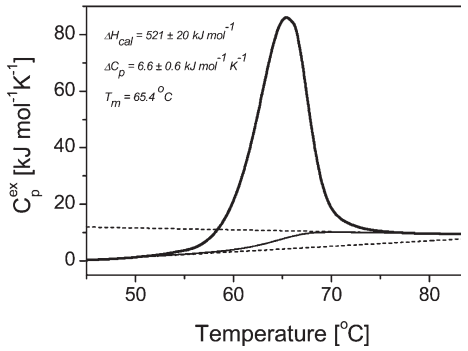

FIGURE 4: Experimental DSC curve of the DraE-sc-ΔSS protein. Experimental dependence of excess heat capacity (C_p^{ex}) on temperature for the DraE-sc-ΔSS protein, obtained at a scanning rate of 1.0 °C/min. The baseline and linear approximations of molar heat capacities of the protein before and after the transition are depicted.

negligible in the transition region. The transition peak is symmetric and does not possess any distortions connected with the exothermic aggregation process. The posttransitional baseline is stable and not affected by any detectable thermal effects of aggregation phenomena (Figure 4). Finally, the calculated cooperativity ratio ($\Delta H_{vH}/\Delta H_{cal}$) is equal to 1.08 and also justifies the use of a two-state reversible model. It is also worth noting that the temperature of DSC peak maxima of DraE-sc-ΔSS varies with a scanning rate between 65.4 and 66.9 °C for scan rates of 1.0 and 2.0 °C/min, respectively, although this effect is rather connected with the problem of establishing the equilibrium at fast scan rates.

DraE-sc-ΔSS is denatured thermally at 65.4 °C, which is more than 20 °C lower than the transition temperature of DraE-sc containing a disulfide bond (*34*). The process of unfolding is connected with a transition enthalpy ΔH_{cal} of 521 ± 20 kJ/mol. Obtained thermograms permit us to determine the apparent molar heat capacity change of unfolding (ΔC_p) of 6.6 ± 0.6 kJ mol^{-1} K^{-1}, which corresponds to a ΔC_p per mole of residue of 44.3 J (mol of residue)$^{-1}$ K^{-1} (Figure 4). This value is suitable for DraE-sc-ΔSS, the protein composed of 149 residues with a molecular mass of ca. 16 kDa (*51*), although the ΔC_p value is much smaller than that published for the Caf1 subunit of the F1 surface antigen of *Y. pestis* (ΔC_p of 8.8 ± 1.3 kJ mol^{-1} K^{-1}) (*30*). To obtain information about the thermodynamic stability of DraE-sc-ΔSS, we calculated the Gibbs free energy change at 25 °C (ΔG_T) connected with the unfolding process according to the following equation:

$$\Delta G_T = \Delta H_{T_m}\left(1 - \frac{T}{T_m}\right) + \Delta C_{pT_m}\left(T - T_m - T\ln\frac{T}{T_m}\right) \quad (1)$$

where ΔH_{T_m} is the reference enthalpy of the transition, corresponding to the T_m, the reference temperature, and ΔC_{pT_m} is the difference between heat capacities of the denatured and native states of the protein at the reference temperature. The obtained ΔG_{25} of 30.0 ± 5.0 kJ/mol correlates well with values determined for type 1 subunit variants that show completely reversible folding equilibria, as a consequence of some structural distortions. The DS_G-$FimH_P$ subunit with a parallel donor strand orientation and the $FimH_P$-DS_C subunit with an antiparallel donor strand from chaperone PapC possess ΔG_{25} values of unfolding of 26.5 and 26.8 ± 2.0 kJ/mol, respectively (*33*). The determined ΔG_{25} of unfolding of DraE-sc-ΔSS is relatively small in contrast to those of other fimbrial subunits with native structure complemented by a specific, canonically oriented antiparallel donor strand. The ΔG_{25} values of unfolding of type 1 subunits range ca. from 50 to 80 kJ/mol (*33*), and the ΔG_{37} of unfolding of the self-complemented Caf1 subunit is ~70−80 kJ/mol (*30*). Although we did not determine the Gibbs free energy change of unfolding for the DraE-sc protein (containing a disulfide bond), we assume that its value may be comparable to that of self-complemented type 1 subunits. This permits us to estimate the stabilizing effect of the disulfide bond in the structure of DraE (and speculatively on other subunits with homologous disulfide bonds) in the range of 40−50 kJ/mol.

DraE-sc is a rather small 16 kDa single-domain structure with an immunoglobulin type fold. Proteins with such a structure usually unfold thermally reversibly as a single cooperative unit. The DraE-sc irreversible denaturation is rather surprising, especially in the context of the Caf1-sc protein that denatures reversibly at a similar temperature and with a similar enthalpy of transition (*30*). DSC experiments performed with DraE-sc-ΔSS clearly show that depletion of the disulfide bond from the structure of DraE-sc renders its features specific to the classical immunoglobulin type proteins from mesophilic organisms (*51*). First, the disulfide bond mutant of DraE-sc unfolds in a reversible fashion. Second, the melting temperature drops from ca. 90 to ca. 65 °C. Third, the standard Gibbs energy of unfolding of DraE-sc-ΔSS is on the level suitable for the statistical globular protein with the weight and fold type represented by DraE-sc (*51*).

Decrease in the Thermal Stability of the DraE-sc-ΔSS Mutant. The FT-IR spectra of DraE-sc-ΔSS are characteristic of β-sheet proteins and are very similar to the spectra of DraE-sc (data not shown) (*34*). This implies that the designed protein construct folds correctly into the nativelike structure. As in previously described experiments, thermal denaturation experiments were performed (*34*). Second derivatives of the amide I′ region of FT-IR spectra were used to obtain the temperature of protein melting and to characterize changes occurring during this process (Figure 5A).

Second derivatives possess bands in positions similar to those of the second derivatives of DraE-sc (*34*). The main differences between second-derivative series of DraE-sc-ΔSS and DraE-sc are the considerably stronger band near 1620 cm^{-1} and the weaker band accompanying it near 1985 cm^{-1}. This can suggest that the mechanism of denaturation of the considered protein is

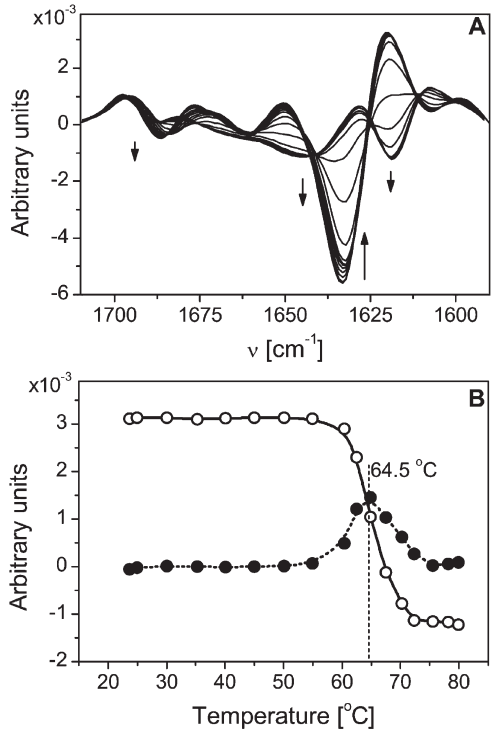

FIGURE 5: Second derivatives and transition curve of DraE-sc-ΔSS. (A) Second derivatives of FT-IR spectra of DraE-sc-ΔSS (the amide I′ band) in temperature range of 23.7−79.9 °C. Arrows indicate changes in curve shape with an increase in temperature. (B) Transition curve determined on the basis of second derivatives of DraE-sc-ΔSS and its derivative with marked temperatures of transition.

considerably different, as DSC results also suggest. The denaturation process is also marked by the presence of a broad second-derivative band with a minimum near 1650 cm^{-1}, corresponding to the unfolded polypeptide chain.

The obtained melting temperature, based on second-derivative intensity at a wavelength of 1620 cm^{-1}, is very similar to the one obtained from DSC studies and is equal to 64.5 °C (Figure 5B). This process seems to be cooperative, as similar denaturation curves drawn on the basis of changes of second-derivative intensities of other wavelengths (data not shown) give almost identical melting temperatures. No other additional transitions are present. The slight decrease in the second-derivative intensity, as mentioned in a previous paper (*34*), might be assigned to a concentration decrease due to thermal expansion of the sample inside the transmission cell.

Unfortunately, no recovery of secondary structure was observed during cooling of the sample (data not shown). This phenomenon might be assigned to the conditions of sample preparation, especially high protein concentrations, necessary to produce a high signal-to-noise ratio. The difference in protein concentrations between both described techniques is sometimes 50-fold, and this difference might be expected to promote another denaturation mechanism in the case of FT-IR-based thermal denaturation experiments.

High Accessibility of Solvent to the DraE-sc-ΔSS Core. The amide II band (maximum at ~1550 cm^{-1}), corresponding mainly to the N−H bending vibrations of the peptide bond, is prone to H−D exchange during protein incubation in D_2O. As described previously, most small globular protein protons, chemically possible of exchanging with a heavier isotope, are exchanged during a short period of time at ambient temperatures (*34*). This

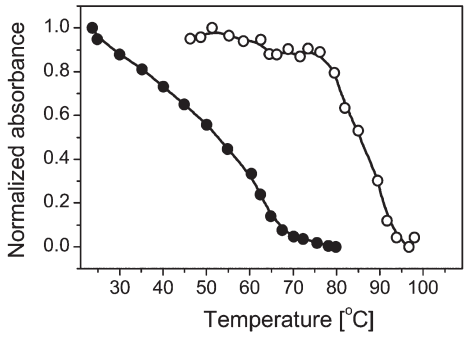

FIGURE 6: Normalized intensity of the amide II band as a function of temperature. The empty circles correspond to the intensities of the residual amide II band of DraE-sc; the filled circles correspond to the intensities of the residual DraE-sc-ΔSS.

causes a shift in the position of the mentioned band to the lower wavenumber (~1450 cm^{-1}). Nevertheless, the residual amide II band might still be visible, if some of the protons are tightly held in the protein interior.

The DraE-sc protein was proven to possess few protons, which are replaced with deuterium only during complete denaturation of the secondary structure (*34*). We proposed a hypothesis in which the disulfide bond played the key role in the observed high thermal stability and rigidity of the protein core, located in a noncanonical position. The reduction experiments showed that even in the presence of a reducing agent (10 mM DTT), denaturation occurs mostly at the same moment, as in the case of the free protein (*34*).

The mutant of DraE-sc lacking a disulfide bond does not possess the same rigidity, as H−D exchange experiments show. In Figure 6, there are two visible curves, characterizing the change in intensity of the amide II band during the temperature increase. It must be mentioned that in the case of DraEsc-ΔSS, the protein was dissolved in D_2O 1 h before the experiment. Both curves were scaled to a common maximum, to better visualize changes in intensities. It is clearly visible that the curve characteristic of DraE-sc is very similar to the standard denaturation curve; meanwhile, the intensity of the DraE-sc-ΔSS amide II band decreases through the whole experiment. This indicates that the presence of the disulfide bridge is crucial to maintaining the high stability of the internal core of this protein.

Molecular Dynamics Analysis of Differential DraE-sc versus DraE-sc-ΔSS Stability. The simulation of the two versions of the DraE-sc protein, the native one containing the disulfide bridge and its double Cys to Ala mutant (DraE-sc-ΔSS), revealed very different behaviors of these two structures. Both proteins are stable at low temperatures and do not undergo any significant structural changes within the range of the simulation time (Figure 7). It clearly demonstrates that the simulation system is well-defined and that removal of the disulfide bond does not influence the structure and dynamics of the protein under the moderate conditions and thus is not itself responsible for the conformational changes in the protein structure.

The significant differences start to emerge in the high-temperature (410 and 473 K) simulations (Figure 7). Protein without the disulfide bond rapidly changes its structure and slowly but systematically drifts away from the native conformation. That is accompanied by the systematic degradation of the secondary structure elements throughout the entire simulation (data not shown), especially in the high-temperature (473 K) dynamics. On the other hand, the protein with the disulfide bridge present is

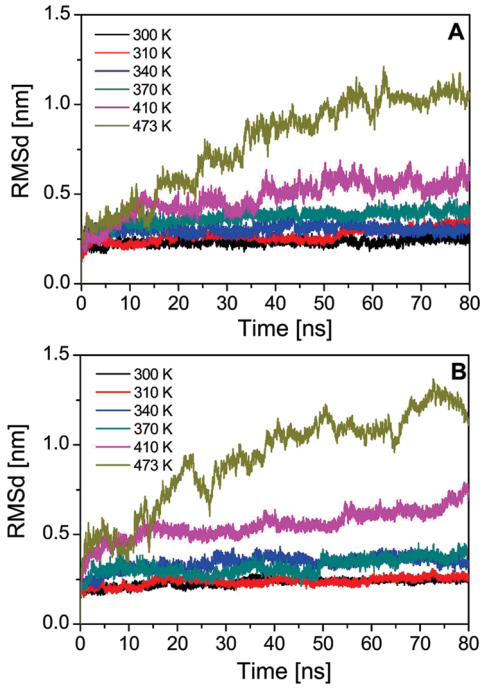

FIGURE 7: Structural changes of DraE-sc and DraE-sc-ΔSS proteins at various temperatures. The rmsd changes of DraE-sc (A) and DraE-sc-ΔSS (B) during the 80 ns molecular dynamics simulation at 300, 310, 340, 370, 410, and 473 K. The rmsd of α-carbons is calculated with respect to their positions in the initial minimized structure of a particular protein.

more resistant to these severe conditions. It is able to keep its native structure almost unchanged for as long as 15 ns, and only after that it gradually, in a stepwise manner, starts to change its conformation (Figure 7). This behavior is confirmed by the change in the secondary structure. For the first 15 ns of the simulation, the secondary structure of this protein remains completely intact, and only after 20 ns do some of the β-strands rapidly disappear (data not shown).

The process of losing the secondary structure elements is bound to the change in the compactness of the protein structure and accessibility of the backbone amide groups to the solvent. Analysis of the ability of particular amide group to create the hydrogen bond with water shows that in high-temperature simulations both DraE-sc-ΔSS and DraE-sc quickly exchange most of their backbone amide hydrogens but the structure possessing the disulfide bridge is able to keep a small number (8−10) of protons shielded from solvent for as long as 20 ns. Interestingly, hydrogens that belong to the NH group of both cysteines are not exposed to the solvent during the entire simulation (Figure 8). There is no such behavior or even similar behavior observed for the structure without the disulfide bridge. In the case of DraE-sc-ΔSS, the number of backbone amide group protons that are not accessible to the solvent shrinks in a fast continuous manner during the simulation and drops completely to zero after 17 ns.

These results indicate that the disulfide bond of the DraE-sc protein has a significant influence on its stability and compactness, especially in the neighborhood of the bond, which is in agreement with the reported resistance of the DraE-sc disulfide bridge to reduction in the presence of a reducing agent (*34*).

DISCUSSION

Subunits of adhesive structures of the chaperone/usher type are characterized by a very high thermodynamic and kinetic

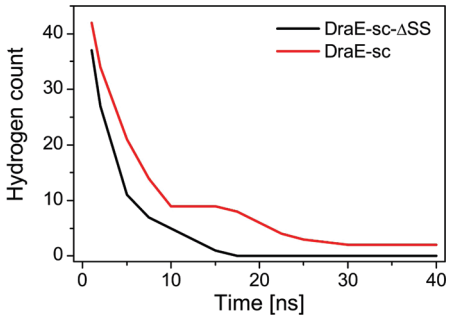

FIGURE 8: Solvent accessibility of DraE-sc vs DraE-sc-ΔSS backbone amide hydrogens. Number of amide hydrogens shielded from solvent during the first 40 ns of simulation. Amide hydrogen is recognized as being shielded from solvent as long as it does not create hydrogen bonds with it.

stability (*30*, *33*, *34*). Most information concerning the subunit stability emerges from analysis of self-complemented forms of these proteins. In these constructs, the Ig-like defective structure of the subunit is complemented by a donor strand introduced as the C-terminal fusion peptide. The self-complemented subunits are generally regarded as the minimal approximation of complex adhesive structures. Fimbrial proteins are among the most thermodynamically stable small globular proteins. Their melting temperature is close to 80−90 °C (85.5 °C for Caf1-sc, 83.4 °C for FimG-sc, and 87.3 °C for DraE-sc), with the corresponding high enthalpy of transition (810 ± 60 kJ/mol for Caf1-sc, 611 kJ/mol for FimG-sc, and 712 ± 46 kJ/mol for DraE-sc) (*30*, *33*, *34*). These data correlate with a high value of the free energy of unfolding (ΔG_{25} = 70−80 kJ/mol for Caf1-sc, and ΔG_{37} = 79.7 ± 2.2 kJ/mol for FimG-sc) (*30*, *33*). Fimbrial subunits are also characterized with a very high kinetic stability. The FimG-sc and DraE-sc proteins unfold with rate constants of 10^{-18} and 10^{-17} s^{-1}, respectively, corresponding to half-lives of unfolding of 10^9 and 10^8 years at 25 °C, respectively (*33*, *34*).

Although many structural data of fimbrial subunits are available, there are no specific structural marks of observed high thermodynamic and kinetic stability. Puorger et al. (*33*) demonstrated that the orientation change of the C-terminal donor strand from antiparallel to parallel resulted in the loss of their infinite kinetic stability, and the standard free energy of unfolding also drops from 70−80 kJ/mol to the value of ~27 kJ/mol. The authors suggest that the observed phenomenon of subunit stability is connected in part with formation of very precise surface complementarity between acceptor cleft binding pockets denoted P1−P5 and residues of the donor strand. Site-directed mutagenesis showed that all residues of the donor strand interacting with binding pockets P1−P5 individually contribute to the kinetic stability of PapG-sc. Zavialov et al. (*24*, *30*) in their elegant work fully define the energetics of F1 antigen formation. The authors delineate that the Caf1 subunit complemented with a specific donor strand is characterized by a very good packing of two β-sheet-forming proteins. The calculated shape correlation statistic (Sc) of the Caf1 protein equals 0.71 (1 denotes a perfect fit) and is comparable to the packing of β-sheets in stable β-barrels (*24*). Similar high Sc values of 0.72 and 0.78 were determined for complexes of PapE and FimG, respectively, with the cognate donor peptide (*23*, *24*, *33*).

In this work, we show that the noncanonical disulfide bond of the DraE protein is an important element responsible for its thermodynamic and kinetic stability. DraE-sc unfolds thermally irreversibly with the thermodynamic and kinetic parameters

presented previously (*34*). The DraE-sc-ΔSS mutant lacking a disulfide bond unfolds reversibly with a melting temperature (T_m) of 65.4 °C, a corresponding enthalpy of transition (ΔH_m) of 521 ± 20 kJ/mol, a change in specific heat capacity of unfolding (ΔC_p) of 6.6 ± 0.6 kJ mol^{-1} K^{-1}, and a calculated standard free energy of unfolding (ΔG_{25}) of 30 ± 5 kJ/mol. The presented data show that deletion of the disulfide bond from the structure of DraE-sc resulted in a protein stability typical for the statistical globular protein from mesophilic organisms (*51*). The DraE-sc protein was also characterized by the specific pattern of proton to deuterium exchange during thermal denaturation, as shown by FT-IR spectroscopy. Most of the amide protons exchange fast before the thermal transition of the protein starts. A small population of protons exchange only at the stage of protein unfolding. These amide protons are probably better sequestered from solvent molecules in the protein scaffold (*34*). This observation is surprising, because DraE-sc has a simple single-domain structure in which it is hard to distinguish some amide protons. This phenomenon vanishes in the case of the mutant DraE-sc lacking a disulfide bond. DraE-sc-ΔSS exchanges protons continuously during sample heating, and the process is finished before the unfolding transition starts. This suggests that the disulfide bond introduced into the DraE-sc scaffold causes some type of restriction which results in different dynamic properties of protein secondary structures during heating. This idea is well-supported by the presented molecular dynamic analysis of the DraE-sc and DraE-sc-ΔSS proteins.

It is worth noting that the disulfide bond of DraE adhesin and protein subunits with homologous bonds possesses unique localization (joining two adjacent β-strands, the beginning of an A1 strand with the end of a B strand), not encountered in any other protein family belonging to the Ig superfamily. This fact additionally supports the idea that the presence of such a positioned disulfide bond is an important stabilizing element of these fimbrial subunits. Additionally, the self-complemented FaeG (F4 fimbriae of *E. coli*), native CssA, and CssB in fimbrial CS6 structures of *E. coli*, which do not possess a disulfide bond in their structures, are denatured at lower temperatures of 62, 75.41, and 70.94 °C, respectively (*44*, *45*). The self-complemented DraD protein, which possesses a disulfide bond connecting strands B and F (canonical localization), is denatured thermally in fully reversible fashion with a melting temperature of 53 °C (data not shown).

In conclusion, we demonstrate that a noncanonical disulfide bond is an important feature in the determination of high thermodynamic and kinetic stability of the DraE protein and potentially other subunits that possess homologous bonds. This mechanism of stabilization is probably widespread in this family of protein subunits building adhesive structures of the chaperone/usher type, as shown by analysis of the disulfide bond distribution. Although it is worth noting that other mechanisms of acquiring high stability by these proteins exist, the well-characterized example of such adhesive subunits is the Caf1 protein of the F1 antigen of *Y. pestis* (*30*).

ACKNOWLEDGMENT

The calorimetric measurements were taken at the laboratory of the Center of Excellence ChemBioFarm at Gdańsk University of Technology, supported by a grant from the European Regional Development Funds. The molecular dynamics calculations were conducted using the resources of the Academic Computer Centre in Gdańsk (TASK).

REFERENCES

1. Hung, D. L., and Hultgren, S. J. (1998) Pilus biogenesis via the chaperone/usher pathway: An integration of structure and function. *J. Struct. Biol. 124*, 201–220.
2. Remaut, H., Tang, C., Henderson, N. S., Pinkner, J. S., Wang, T., Hultgren, S. J., Thanassi, D. G., Waksman, G., and Li, H. (2008) Fiber formation across the bacterial outer membrane by the chaperone/usher pathway. *Cell 133*, 640–652.
3. Thanassi, D. G., and Hultgren, S. J. (2000) Assembly of complex organelles: Pilus biogenesis in Gram-negative bacteria as a model system. *Methods 20*, 111–126.
4. Lindler, L. E., and Tall, B. D. (1993) *Yersinia pestis* pH 6 antigen forms fimbriae and is induced by intracellular association with macrophages. *Mol. Microbiol. 8*, 311–324.
5. Zavialov, A. V., Kersley, J., Korpela, T., Zav'yalov, V. P., MacIntyre, S., and Knight, S. D. (2002) Donor strand complementation mechanism in the biogenesis of non-pilus systems. *Mol. Microbiol. 45*, 983–995.
6. Swanson, T. N., Bilge, S. S., Nowicki, B., and Moseley, S. L. (1991) Molecular structure of the Dr adhesin: Nucleotide sequence and mapping of receptor-binding domain by use of fusion constructs. *Infect. Immun. 59*, 261–268.
7. Piatek, R., Zalewska, B., Kolaj, O., Ferens, M., Nowicki, B., and Kur, J. (2005) Molecular aspects of biogenesis of *Escherichia coli* Dr Fimbriae: Characterization of DraB-DraE complexes. *Infect. Immun. 73*, 135–145.
8. Cota, E., Jones, C., Simpson, P., Altroff, H., Anderson, K. L., du Merle, L., Guignot, J., Servin, A., Le Bouguénec, C., Mardon, H., and Matthews, S. (2006) The solution structure of the invasive tip complex from Afa/Dr fibrils. *Mol. Microbiol. 62*, 356–366.
9. Anderson, K. L., Billington, J., Pettigrew, D., Cota, E., Simpson, P., Roversi, P., Chen, H. A., Urvil, P., du Merle, L., Barlow, P. N., Medof, M. E., Smith, R. A., Nowicki, B., Le Bouguénec, C., Lea, S. M., and Matthews, S. (2004) An atomic resolution model for assembly, architecture, and function of the Dr adhesins. *Mol. Cell 15*, 647–657.
10. Zavialov, A., Zav'yalova, G., Korpela, T., and Zav'yalov, V. (2007) FGL chaperone-assembled fimbrial polyadhesins: Anti-immune armament of Gram-negative bacterial pathogens. *FEMS Microbiol. Rev. 31*, 478–514.
11. Nowicki, B., Moulds, J., Hull, R., and Hull, S. (1988) A hemagglutinin of uropathogenic *Escherichia coli* recognizes the Dr blood group antigen. *Infect. Immun. 56*, 1057–1060.
12. Pham, T., Kaul, A., Hart, A., Goluszko, P., Moulds, J., Nowicki, S., Lublin, D. M., and Nowicki, B. J. (1995) dra-related X adhesins of gestational pyelonephritis-associated *Escherichia coli* recognize SCR-3 and SCR-4 domains of recombinant decay-accelerating factor. *Infect. Immun. 63*, 1663–1668.
13. Selvarangan, R., Goluszko, P., Singhal, J., Carnoy, C., Moseley, S., Hudson, B., Nowicki, S., and Nowicki, B. (2004) Interaction of Dr adhesin with collagen type IV is a critical step in *Escherichia coli* renal persistence. *Infect. Immun. 72*, 4827–4835.
14. Servin, A. L. (2005) Pathogenesis of Afa/Dr diffusely adhering *Escherichia coli*. *Int. J. Med. Microbiol. 295*, 471–478.
15. Korotkova, N., Yarova-Yarovaya, Y., Tchesnokova, V., Yazvenko, N., Carl, M. A., Stapleton, A. E., and Moseley, S. L. (2008) *Escherichia coli* DraE adhesin-associated bacterial internalization by epithelial cells is promoted independently by decay-accelerating factor and carcinoembryonic antigen-related cell adhesion molecule binding and does not require the DraD invasin. *Infect. Immun. 76*, 3869–3880.
16. Jouve, M., Garcia, M. I., Courcoux, P., Labigne, A., Gounon, P., and Le Bouguénec, C. (1997) Adhesion to and invasion of HeLa cells by pathogenic *Escherichia coli* carrying the afa-3 gene cluster are mediated by the AfaE and AfaD proteins, respectively. *Infect. Immun. 56*, 4082–4089.
17. Gounon, P., Jouve, M., and Le Bouguenec, C. (2000) Immunocytochemistry of the AfaE adhesin and AfaD invasin produced by pathogenic *Escherichia coli* strains during interaction of the bacteria with HeLa cells by high resolution scanning electron microscopy. *Microbes Infect. 2*, 359–365.
18. Zalewska, B., Piątek, R., Bury, K., Samet, A., Nowicki, B., Nowicki, S., and Kur, J. (2005) A surface-exposed DraD protein of uropathogenic *Escherichia coli* bearing Dr fimbriae may be expressed and secreted independently from DraC usher and DraE adhesion. *Microbiology 151*, 2477–2486.
19. Sauer, F. G., Futterer, K., Pinkner, J. S., Dodson, K. W., Hultgren, S. J., and Waksman, G. (1999) Structural basis of chaperone function and pilus biogenesis. *Science 285*, 1058–1061.

20. Sauer, F. G., Barnhart, M., Choudhury, D., Knight, S. D., Waksman, G., and Hultgren, S. J. (2000) Chaperone-assisted pilus assembly and bacterial attachment. *Curr. Opin. Struct. Biol. 10*, 548–556.
21. Vetsch, M., Erilov, D., Molière, N., Nishiyama, M., Ignatov, O., and Glockshuber, R. (2006) Mechanism of fibre assembly through the chaperone-usher pathway. *EMBO Rep. 7*, 734–738.
22. Choudhury, D., Thompson, A., Stojanoff, V., Langermann, S., Pinkner, J., Hultgren, S. J., and Knight, S. D. (1999) X-ray structure of the FimC-FimH chaperone-adhesin complex from uropathogenic *Escherichia coli*. *Science 285*, 1061–1066.
23. Sauer, F. G., Pinkner, J. S., Waksman, G., and Hultgren, S. J. (2002) Chaperone priming of pilus subunits facilitates a topological transition that drives fiber formation. *Cell 111*, 543–551.
24. Zavialov, A. V., Berglund, J., Pudney, A. F., Fooks, L. J., Ibrahim, T. M., MacIntyre, S., and Knight, S. D. (2003) Structure and biogenesis of the capsular F1 antigen from *Yersinia pestis*: Preserved folding energy drives fiber formation. *Cell 113*, 587–596.
25. Korotkova, N., Le Trong, I., Samudrala, R., Korotkov, K., Van Loy, C. P., Bui, A. L., Moseley, S. L., and Stenkamp, R. E. (2006) Crystal structure and mutational analysis of the DaaE adhesin of *Escherichia coli*. *J. Biol. Chem. 281*, 22367–22377.
26. Verger, D., Bullitt, E., Hultgren, S. J., and Waksman, G. (2007) Crystal structure of the P pilus rod subunit PapA. *PLoS Pathog. 3*, 73.
27. Gossert, A. D., Bettendorff, P., Puorger, C., Vetsch, M., Herrmann, T., Glockshuber, R., and Wüthrich, K. (2008) NMR structure of the *Escherichia coli* type 1 pilus subunit FimF and its interactions with other pilus subunits. *J. Mol. Biol. 375*, 752–763.
28. Hung, D. L., Knight, S. D., Woods, R. M., Pinkner, J. S., and Hultgren, S. J. (1996) Molecular basis of two subfamilies of immunoglobulin-like chaperones. *EMBO J. 15*, 3792–3805.
29. Barnhart, M. M., Pinkner, J. S., Soto, G. E., Sauer, F. G., Langermann, S., Waksman, G., Frieden, C., and Hultgren, S. J. (2000) PapD-like chaperones provide the missing information for folding of pilin proteins. *Proc. Natl. Acad. Sci. U.S.A. 97*, 7709–7714.
30. Zavialov, A. V., Tischenko, V. M., Fooks, L. J., Brandsdal, B. O., Aqvist, J., Zav'yalov, V. P., Macintyre, S., and Knight, S. D. (2005) Resolving the energy paradox of chaperone/usher-mediated fibre assembly. *Biochem. J. 389*, 685–694.
31. Vetsch, M., Sebbel, P., and Glockshuber, R. (2002) Chaperone-independent folding of type 1 pilus domains. *J. Mol. Biol. 322*, 827–840.
32. Erilov, D., Puorger, C., and Glockshuber, R. (2007) Quantitative analysis of nonequilibrium, denaturant-dependent protein folding transitions. *J. Am. Chem. Soc. 129*, 8938–8939.
33. Puorger, C., Eidam, O., Capitani, G., Erilov, D., Grütter, M. G., and Glockshuber, R. (2008) Infinite kinetic stability against dissociation of supramolecular protein complexes through donor strand complementation. *Structure 16*, 631–642.
34. Piątek, R., Bruździak, P., Zalewska-Piątek, B., Kur, J., and Stangret, J. (2009) The preclusion of irreversible destruction of Dr adhesin structures by a high activation barrier for unfolding stage of the fimbrial DraE subunit. *Biochemistry 48*, 11807–11816.
35. Finn, R. D., Tate, J., Mistry, J., Coggill, P. C., Sammut, S. J., Hotz, H. R., Ceric, G., Forslund, K., Eddy, S. R., Sonnhammer, E. L., and Bateman, A. (2008) The Pfam protein families database. *Nucleic Acids Res. 36*, 281–288.
36. Tatusov, R. L., Fedorova, N. D., Jackson, J. D., Jacobs, A. R., Kiryutin, B., Koonin, E. V., Krylov, D. M., Mazumder, R., Mekhedov, S. L., Nikolskaya, A. N., Rao, B. S., Smirnov, S., Sverdlov, A. V., Vasudevan, S., Wolf, Y. I., Yin, J. J., and Natale, D. A. (2003) The COG database: An updated version includes eukaryotes. *BMC Bioinf. 4*, 41.
37. Nuccio, S. P., and Bäumler, A. J. (2007) Evolution of the chaperone/usher assembly pathway: Fimbrial classification goes Greek. *Microbiol. Mol. Biol. Rev. 71*, 551–575.
38. Hess, B., Kutzner, C., van der Spoel, D., and Lindahl, E. (2008) GROMACS 4: Algorithms for highly efficient, load-balanced, and scalable molecular simulation. *J. Chem. Theory Comput. 4*, 435–447.
39. Halaby, D. M., Poupon, A., and Mornon, J. P. (1999) The immunoglobulin fold family: Sequence analysis and 3D structure comparisons. *Protein Eng. 12*, 563–571.
40. Verger, D., Miller, E., Remaut, H., Waksman, G., and Hultgren, S. (2006) Molecular mechanism of P pilus termination in uropathogenic *Escherichia coli*. *EMBO Rep. 12*, 1228–1232.
41. Tomaras, A. P., Dorsey, C. W., Edelmann, R. E., and Actis, L. A. (2003) Attachment to and biofilm formation on abiotic surfaces by *Acinetobacter baumannii*: Involvement of a novel chaperone-usher pili assembly system. *Microbiology 149*, 3473–3484.
42. Van Molle, I., Moonens, K., Garcia-Pino, A., Buts, L., De Kerpel, M., Wyns, L., Bouckaert, J., and De Greve, H. (2009) Structural and thermodynamic characterization of pre- and postpolymerization states in the F4 fimbrial subunit FaeG. *J. Mol. Biol. 394*, 957–967.
43. Jedrzejczak, R., Dauter, Z., Dauter, M., Piatek, R., Zalewska, B., Mróz, M., Bury, K., Nowicki, B., and Kur, J. (2006) Structure of DraD invasin from uropathogenic *Escherichia coli*: A dimer with swapped β-tails. *Acta Crystallogr. D62*, 157–164.
44. Remaut, H., Rose, R. J., Hannan, T. J., Hultgren, S. J., Radford, S. E., Ashcroft, A. E., and Waksman, G. (2006) Donor-strand exchange in chaperone-assisted pilus assembly proceeds through a concerted β strand displacement mechanism. *Mol. Cell 22*, 831–842.
45. Ghosal, A., Bhowmick, R., Banerjee, R., Ganguly, S., Yamasaki, S., Ramamurthy, T., Hamabata, T., and Chatterjee, N. S. (2009) Characterization and studies of the cellular interaction of native colonization factor CS6 purified from a clinical isolate of enterotoxigenic *Escherichia coli*. *Infect. Immun. 77*, 2125–2135.
46. Jaswal, S. S., Sohl, J. L., Davis, J. H., and Agard, D. A. (2002) Energetic landscape of α-lytic protease optimizes longevity through kinetic stability. *Nature 415*, 343–346.
47. Rupley, J. A. (1967) Susceptibility to attack by proteolytic enzymes. *Methods Enzymol. 11*, 905–917.
48. Manning, M., and Colón, W. (2004) Structural basis of protein kinetic stability: Resistance to sodium dodecyl sulfate suggests a central role for rigidity and a bias toward β-sheet structure. *Biochemistry 43*, 11248–11254.
49. Eshdat, Y., Silverblatt, F. J., and Sharon, N. (1981) Dissociation and reassembly of *Escherichia coli* type 1 pili. *J. Bacteriol. 148*, 308–314.
50. Orndorff, P. E., and Falkow, S. (1984) Organization and expression of genes responsible for type 1 piliation in *Escherichia coli*. *J. Bacteriol. 159*, 736–744.
51. Makhatadze, G. I., and Privalov, P. L. (1995) Energetics of protein structure. *Adv. Protein Chem. 47*, 307–425.
52. Shatsky, M., Nussinovk, R., and Wolfson, H. J. (2004) A method for simultaneous alignment of multiple protein structures. *Proteins 56*, 143–156.